Supporting Information

Magnetic behaviours dominated by the interplay of magnetic anisotropy and exchange coupling in the local Co^{II}_7 discs

En-Cui Yang,*[, a] Zhong-Yi Liu,[a] Lei Zhang,[a] Na Yang,[a] Xiao-Jun Zhao*[, a, b]

Table S1. Selected bond distances (Å) and angles (°) for **1** [a]

Co(1)–O(9)	1.998(3)	Co(1)–O(13)	2.101(3)
Co(1)–O(22)	2.004(3)	Co(1)–O(6)	2.176(3)
Co(1)–N(6)	2.042(3)	Co(1)–O(26)	2.285(4)
Co(2)–O(3)	2.006(3)	Co(2)–O(17)	2.094(3)
Co(2)–O(21)	2.038(3)	Co(2)–O(25)	2.171(3)
Co(2)–N(7)	2.077(3)	Co(2)–O(6)	2.208(3)
Co(3)–O(14)	2.073(3)	Co(3)–O(22)	2.105(3)
Co(3)–O(24)	2.099(3)	Co(3)–O(30)$^{\#1}$	2.122(3)
Co(3)–O(15)$^{\#2}$	2.101(2)	Co(3)–O(10)	2.170(3)
Co(4)–O(23)	1.961(3)	Co(4)–O(20)$^{\#3}$	2.075(3)
Co(4)–O(11)$^{\#1}$	1.980(3)	Co(4)–O(7)$^{\#1}$	2.183(3)
Co(4)–N(1)	2.016(3)	Co(5)–O(5)	2.086(3)
Co(5)–O(22)	2.061(3)	Co(5)–O(24)	2.105(3)
Co(5)–O(23)	2.070(3)	Co(5)–O(8)$^{\#1}$	2.114(3)
Co(5)–O(21)	2.081(3)	Co(6)–O(16)$^{\#2}$	2.070(3)
Co(6)–O(24)	1.968(3)	Co(6)–O(7)$^{\#1}$	2.165(3)
Co(6)–O(31)$^{\#1}$	1.997(3)	Co(6)–N(2)	2.028(3)
Co(7)–O(18)	2.072(2)	Co(7)–O(4)	2.117(3)
Co(7)–O(21)	2.082(3)	Co(7)–O(23)	2.129(3)
Co(7)–O(19)$^{\#3}$	2.104(3)	Co(7)–O(12)$^{\#1}$	2.181(3)
O(9)–Co(1)–O(22)	99.00(11)	O(9)–Co(1)–O(13)	90.49(11)
O(9)–Co(1)–O(6)	83.65(11)	O(22)–Co(1)–O(13)	90.01(11)
O(9)–Co(1)–O(2)	81.10(14)	O(22)–Co(1)–N(6)	101.01(12)
N(6)–Co(1)–O(6)	89.40(11)	O(22)–Co(1)–O(6)	96.17(10)
N(6)–Co(1)–O(13)	94.31(11)	O(13)–Co(1)–O(2)	83.19(14)
N(6)–Co(1)–O(2)	79.60(15)	O(6)–Co(1)–O(2)	90.60(14)
O(3)–Co(2)–O(21)	96.84(11)	O(21)–Co(2)–N(7)	96.59(11)
O(3)–Co(2)–O(17)	90.09(11)	O(21)–Co(2)–O(17)	90.68(10)
N(7)–Co(2)–O(17)	93.14(11)	N(7)–Co(2)–O(25)	84.13(12)
O(3)–Co(2)–O(25)	82.60(12)	O(17)–Co(2)–O(25)	86.88(12)
O(21)–Co(2)–O(6)	91.28(10)	O(3)–Co(2)–O(6)	87.15(11)
O(25)–Co(2)–O(6)	91.14(11)	N(7)–Co(2)–O(6)	89.16(11)

O(24)–Co(3)–O(22)	79.15(10)	O(24)–Co(3)–O(15)$^{\#2}$	94.35(10)
O(14)–Co(3)–O(15)$^{\#2}$	92.62(10)	O(14)–Co(3)–O(22)	94.19(10)
O(14)–Co(3)–O(30)$^{\#1}$	85.79(11)	O(24)–Co(3)–O(30)$^{\#1}$	97.80(11)
O(15)$^{\#2}$–Co(3)–O(30)$^{\#1}$	86.71(11)	O(24)–Co(3)–O(10)	93.31(11)
O(22)–Co(3)–O(30)$^{\#1}$	89.11(11)	O(15)$^{\#2}$–Co(3)–O(10)	82.42(10)
O(22)–Co(3)–O(10)	102.90(10)	O(14)–Co(3)–O(10)	84.42(11)
O(23)–Co(4)–O(7)$^{\#1}$	95.96(11)	O(23)–Co(4)–O(11)$^{\#1}$	106.86(11)
O(23)–Co(4)–N(1)	114.84(12)	O(23)–Co(4)–O(20)$^{\#3}$	95.87(11)
N(1)–Co(4)–O(7)$^{\#1}$	84.24(11)	N(1)–Co(4)–O(20)$^{\#3}$	94.37(11)
O(11)$^{\#1}$–Co(4)–N(1)	137.47(12)	O(11)$^{\#1}$–Co(4)–O(7)$^{\#1}$	83.54(11)
O(11)$^{\#1}$–Co(4)–O(20)$^{\#3}$	89.23(12)	O(21)–Co(5)–O(8)$^{\#1}$	86.02(10)
O(22)–Co(5)–O(21)	101.90(10)	O(21)–Co(5)–O(5)	93.34(11)
O(22)–Co(5)–O(24)	80.02(10)	O(23)–Co(5)–O(24)	97.17(10)
O(22)–Co(5)–O(5)	92.72(11)	O(23)–Co(5)–O(8)$^{\#1}$	93.13(11)
O(22)–Co(5)–O(8)$^{\#1}$	87.01(11)	O(23)–Co(5)–O(21)	80.91(10)
O(5)–Co(5)–O(24)	85.77(11)	O(24)–Co(6)–O(31)$^{\#1}$	110.57(11)
O(24)–Co(5)–O(8)$^{\#1}$	94.89(11)	O(24)–Co(6)–O(16)$^{\#2}$	94.06(11)
O(24)–Co(6)–N(2)	112.40(12)	O(31)$^{\#1}$–Co(6)–O(16)$^{\#2}$	88.76(11)
O(31)$^{\#1}$–Co(6)–N(2)	136.70(12)	N(2)–Co(6)–O(16)$^{\#2}$	93.30(11)
O(24)–Co(6)–O(7)$^{\#1}$	93.17(11)	O(31)$^{\#1}$–Co(6)–O(7)$^{\#1}$	87.85(11)
N(2)–Co(6)–O(7)$^{\#1}$	84.78(11)	O(19)$^{\#3}$–Co(7)–O(4)	84.11(11)
O(18)–Co(7)–O(19)$^{\#3}$	93.37(10)	O(21)–Co(7)–O(23)	79.52(10)
O(18)–Co(7)–O(4)	88.94(10)	O(19)$^{\#3}$–Co(7)–O(23)	92.83(10)
O(21)–Co(7)–O(4)	102.37(11)	O(18)–Co(7)–O(21)	94.76(10)
O(4)–Co(7)–O(23)	87.94(10)	O(23)–Co(7)–O(12)$^{\#1}$	100.64(10)
O(18)–Co(7)–O(12)$^{\#1}$	84.00(10)	O(19)$^{\#3}$–Co(7)–O(12)$^{\#1}$	81.75(10)
O(21)–Co(7)–O(12)$^{\#1}$	92.78(10)		

[a] Symmetry codes: $^{\#1}$ $1 - x, y - 1/2, 1/2 - z$; $^{\#2}$ $-x, -y, -z$; $^{\#3}$ $2 - x, -y, 1 - z$.

Table S2. Hydrogen-bonding parameters (Å, deg) for **1** and **2** [a]

D–H···A	*d* (D–H)	*d* (H···A)	*d* (D..A)	∠DHA
1				
N10–H10B···O29A[#1]	0.86	2.06	2.898(8)	165.2
N5–H5B···O28	0.86	2.14	2.949(6)	158.1
O21–H21···N9[#2]	0.82	2.46	3.275(1)	178.0
O24–H24A···N4[#1]	0.82	2.36	3.178(2)	174.0
2				
O7W–H7WA···O4[#1]	0.84	2.26	2.889(17)	131.8
O7W–H7WB ···N1[#2]	0.84	1.74	2.57(3)	166.8
O7W–H7WB ···N7[#3]	0.84	1.92	2.73(14)	161.3

[a] Symmetry codes: for **1** [#1] x–1, 1/2– y, z–1/2; [#2] 1 – x, – y, 1 – z. For **2**: [#1] 2 – x, 1 – y, 1 – z; [#2] x + 1/2, y + 1/2, z + 1/2; [#3] x + 1/2, 3/2 – y, z + 1/2.

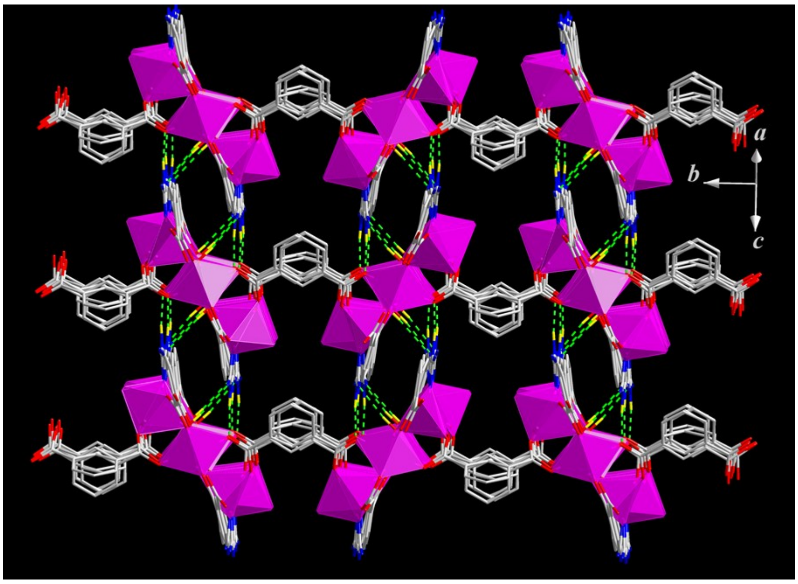

Fig. S1 3D supramolecular network of **1** formed by hydrogen-bonding interactions.

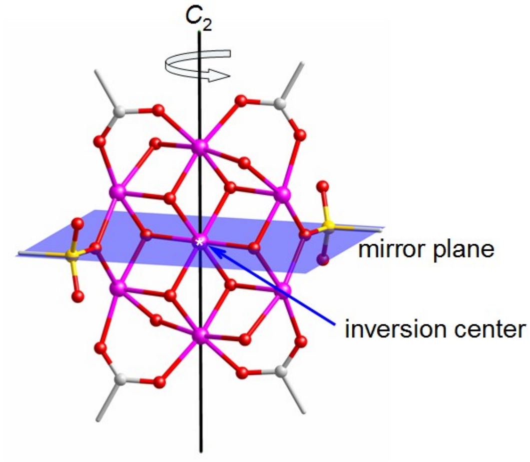

Fig. S2 Crystallographic symmetry in the local Co^{II}_7 disc of **2**.

Table S3. Selected bond distance (Å) and angles (°) for **2** [a]

Co(1)–O(5)	2.097(11)	Co(3)–O(5)$^{\#3}$	2.061(10)
Co(1)–O(6)	2.105(13)	Co(3)–O(2)$^{\#6}$	2.067(11)
Co(2)–O(5)	2.018(11)	Co(3)–N(3)	2.17(2)
Co(2)–O(1)$^{\#4}$	2.086(12)	Co(3)–O(3)	2.209(12)
Co(2)–O(7)	2.227(11)	Co(3)–O(7)$^{\#3}$	2.301(11)
Co(3)–O(6)	2.044(9)	N(9)–Co(3)$^{\#1}$	1.976(13)
O(5)$^{\#1}$–Co(1)–O(5)$^{\#2}$	180.0(4)	O(6)–Co(3)–O(5)$^{\#3}$	83.3(5)
O(5)$^{\#1}$–Co(1)–O(5)	100.9(6)	O(6)–Co(3)–O(2)$^{\#6}$	167.8(5)
O(5)$^{\#2}$–Co(1)–O(5)	79.1(6)	O(5)$^{\#3}$–Co(3)–O(2)$^{\#6}$	91.1(5)
O(5)$^{\#2}$–Co(1)–O(6)	80.9(4)	O(6)–Co(3)–N(3)	88.8(9)
O(5)–Co(1)–O(6)	99.1(4)	O(5)$^{\#3}$–Co(3)–N(3)	166.7(8)
O(6)–Co(1)–O(6)$^{\#3}$	180.0	O(2)$^{\#6}$–Co(3)–N(3)	98.6(8)
O(5)–Co(2)–O(5)$^{\#2}$	82.9(6)	O(6)–Co(3)–O(3)	81.3(5)
O(5)–Co(2)–O(1)$^{\#4}$	168.9(4)	O(5)$^{\#3}$–Co(3)–O(3)	86.4(5)
O(5)$^{\#2}$–Co(2)–O(1)$^{\#4}$	91.1(5)	O(2)$^{\#6}$–Co(3)–O(3)	109.2(5)
O(1)$^{\#4}$–Co(2)–O(1)$^{\#5}$	96.2(7)	N(3)–Co(3)–O(3)	81.8(10)
O(1)$^{\#4}$–Co(2)–O(7)$^{\#2}$	85.2(5)	O(6)–Co(3)–O(7)$^{\#3}$	87.0(5)
O(5)–Co(2)–O(7)	87.3(4)	O(5)$^{\#3}$–Co(3)–O(7)$^{\#3}$	84.3(4)
O(5)$^{\#2}$–Co(2)–O(7)	85.2(4)	O(2)$^{\#6}$–Co(3)–O(7)$^{\#3}$	81.7(4)
O(1)$^{\#4}$–Co(2)–O(7)	101.6(4)	N(3)–Co(3)–O(7)$^{\#3}$	106.0(10)
O(7)$^{\#2}$–Co(2)–O(7)	170.0(6)	O(3)–Co(3)–O(7)$^{\#3}$	165.9(4)

[a] Symmetry codes: $^{\#1}$ x, $1-y$, z; $^{\#2}$ $1-x$, y, $1-z$; $^{\#3}$ $1-x$, $1-y$, $1-z$; $^{\#4}$ $3/2-x$, $y+1/2$, $1/2-z$; $^{\#5}$ $x-1/2$, $y+1/2$, $z+1/2$; $^{\#6}$ $3/2-x$, $1/2-y$, $1/2-z$.

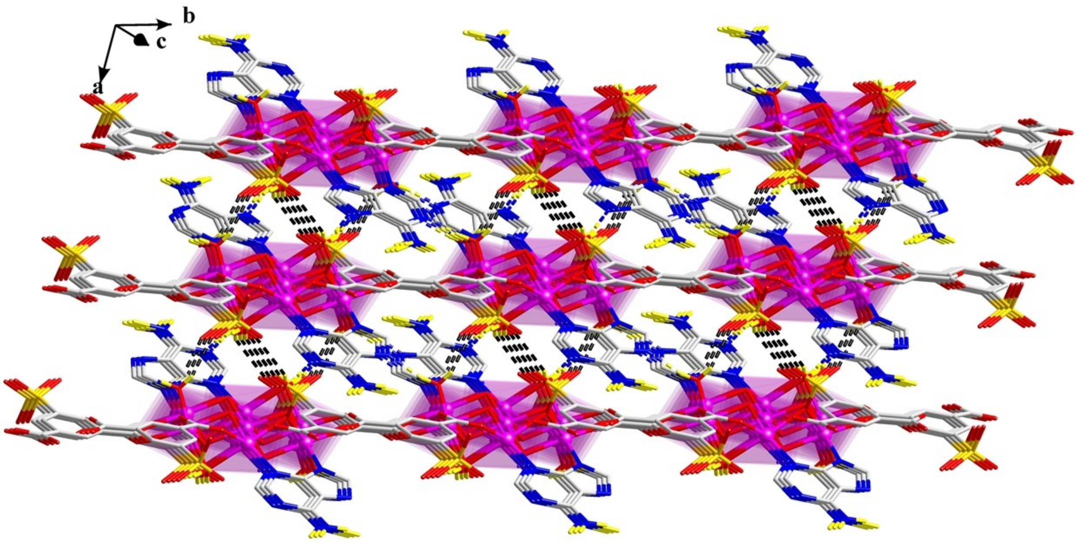

Fig. S3 3D supramolecular network of **2** generated by hydrogen-bonding interactions.

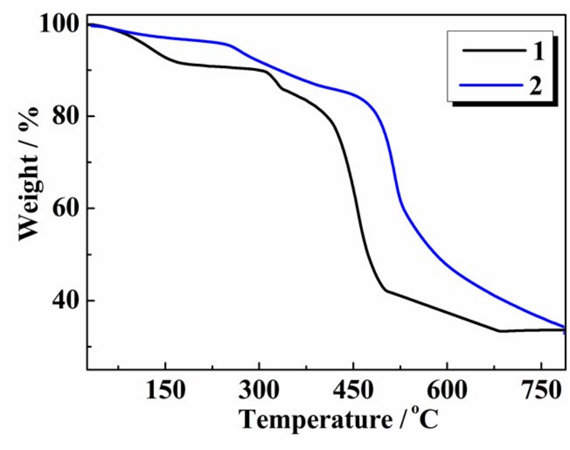

Fig. S4 TG curves for **1** and **2**.

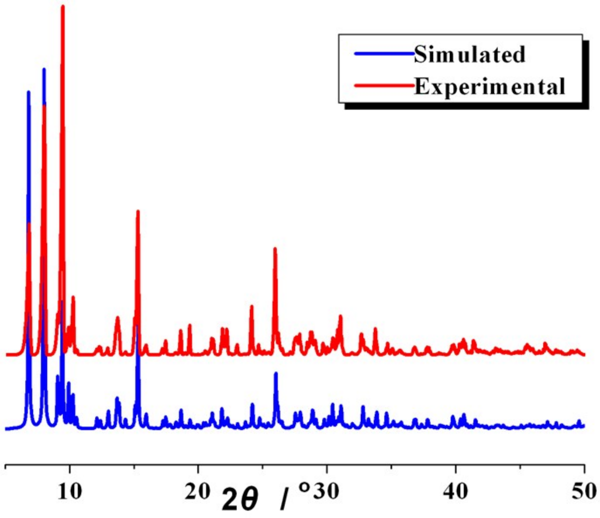

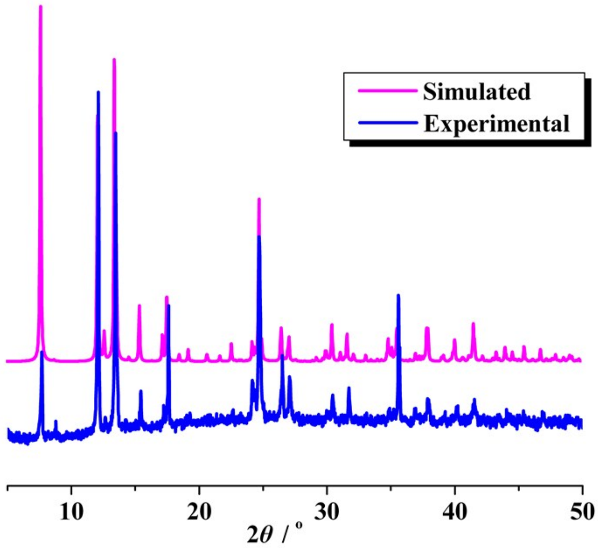

Fig. S5 Simulated and experimental PXRD patterns for **1** (top) and **2** (bottom).

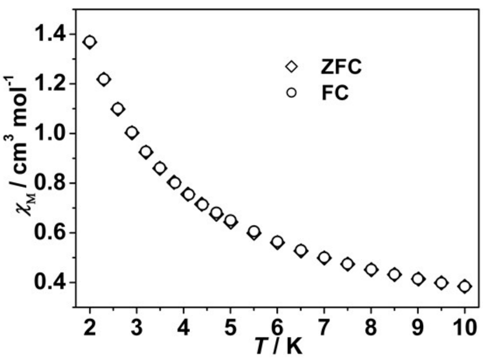

Fig. S6 FC and ZFC magnetizations for **1** at 50.0 Oe dc field.

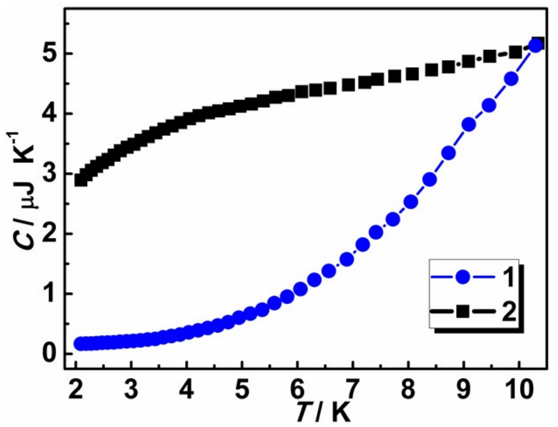

Fig. S7 Temperature-dependent heat capacity for **1** and **2** measured at zero dc field.

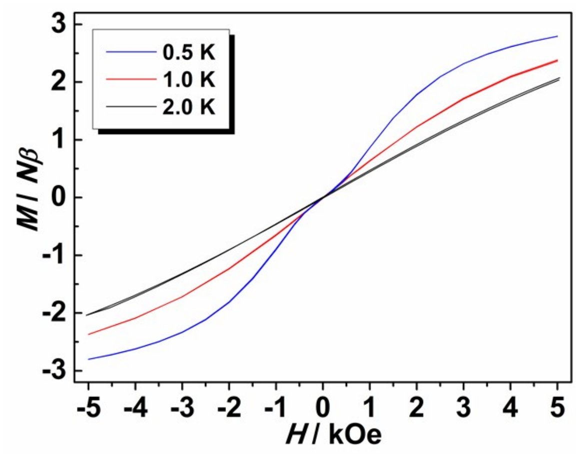

Fig. S8 Magnetization (*M*) *vs*. applied dc field (*H*) hysteresis loops for **1** at the indicated temperatures.

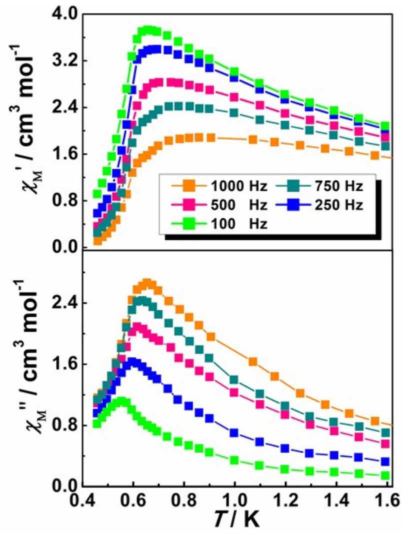

Fig. S9 Temperature dependence of real (χ') and imaginary (χ'') components of the ac susceptibility of **1** in zero dc field with an oscillating field of 3.5 Oe over frequencies of 100−1500 Hz.

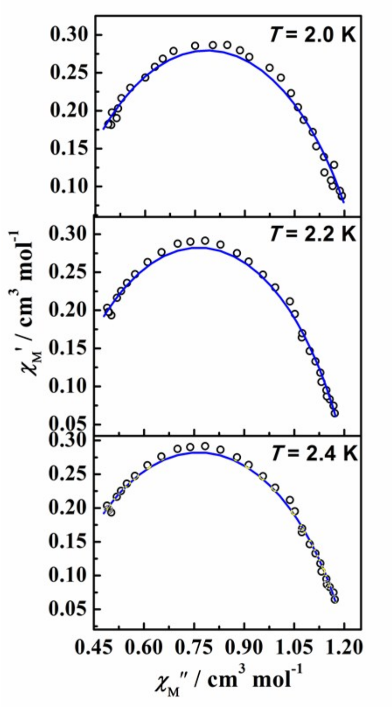

Fig. S10 Cole−Cole plots of **1** at different temperatures.

Table S4. Parameters obtained by fitting the ac magnetic susceptibilities between 2.0 and 2.4 K with generalized Debye-model for **1**.

T / K	χ_0 / cm^3 mol^{-1}	χ_∞/ cm^3 mol^{-1}	τ (s)	α	R
2.0 K	1.24	0.32	6×10^{-4}	0.31	5.5×10^{-3}
2.2 K	1.21	0.32	5×10^{-4}	0.28	5.8×10^{-3}
2.4 K	1.17	0.28	3×10^{-4}	0.25	2.1×10^{-3}

$R = \sum[(\chi'_{obs} - \chi'_{cal})^2 + (\chi''_{obs} - \chi''_{cal})^2]/\sum(\chi'^2_{obs} + \chi''^2_{obs})$

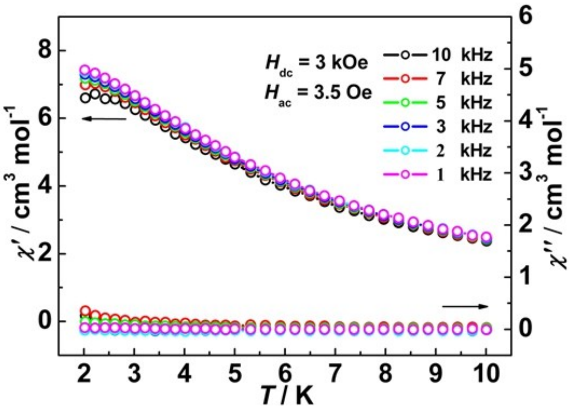

Fig. S11 Temperature dependence of real (χ') and imaginary (χ'') components of the ac susceptibility for **2** under H_{dc} = 3000 and H_{ac}=3.5 Oe over the frequencies of 1–10 kHz.